

**NISTIR 6191**

---

---

**Demonstration Of Biodegradable, Environmentally  
Safe, Non-Toxic Fire Suppression Liquids**

---

---

**Daniel Madrzykowski  
David W. Stroup, Editors**

**July 1998**



**U.S. Department of Commerce  
Technology Administration  
National Institute of Standards and Technology  
Gaithersburg, MD 20899**



*Prepared for:*  
**Federal Emergency Management Agency  
U.S. Fire Administration  
Emmitsburg, MD 21727-8998**



**NISTIR 6191**

---

---

# Demonstration Of Biodegradable, Environmentally Safe, Non-Toxic Fire Suppression Liquids

---

---

**Daniel Madrzykowski  
David W. Stroup, Editors**

July 1998



**U.S. Department of Commerce**  
William M. Daley, *Secretary*  
**Technology Administration**  
Gary R. Bachula, *Under Secretary for Technology*  
National Institute of Standards and Technology  
Raymond G. Kammer, *Director*



*Prepared for:*  
**Federal Emergency Management Agency**  
James Lee Witt, *Director*  
**U.S. Fire Administration**  
Carrye B. Brown, *Administrator*



**CHAPTER 2**  
**FIRE FIGHTING PROPERTIES**

David W. Stroup,  
Daniel Madrzykowski  
and  
Matthew J. Bishop  
National Institute of Standards and Technology  
Building and Fire Research Laboratory  
Fire Safety Engineering Division  
Large Fire Research  
Gaithersburg, Maryland

# FIRE FIGHTING PROPERTIES

## 2.1 Introduction

Water uses several different mechanisms to suppress and extinguish fires: fuel cooling, flame cooling, oxygen displacement and reduction of radiation feedback to the fuel. Laboratory experiments were conducted to determine which of these mechanisms play dominant roles in the suppression of Class A fires and which mechanisms are enhanced by addition of the agents. These laboratory-scale experiments have the advantage of being able to examine individual mechanisms one at a time. The sections in this chapter address experiments conducted to quantify specific heat, droplet size, fuel cooling and penetration, and fuel surface contact.

## 2.2 Specific Heat

Specific heat can be used as a means to examine the cooling capability or ability to absorb heat of fire suppression agents. As noted in Chapter 1, “water has a very high latent heat of vaporization per unit volume, at least four times as high as that of any other non-flammable liquid”, 2254.8 kJ/kg (970.3 Btu/lb) [1]. The latent heat of vaporization of water is the amount of heat absorbed by 1 kg (2.2 lb) of water when changing from a liquid to a gas, at atmospheric pressure. Another measure of a material’s ability to absorb heat is specific heat. Specific heat is the amount of heat required to raise the temperature of a unit mass of a material one degree at constant pressure. Typically, water has a specific heat of 4.186 kJ/kg/K or 1 Btu/lb/F. This is the amount of thermal energy required to raise the temperature of 1 kg (2.2 lb) of water 1 °C (1.8 °F) [2].

### 2.2.1 Experimental Procedure

The objective of these experiments was to develop data on the specific heat capacities at constant pressure,  $c_p$ , for various aqueous fire fighting agents near 298.15 K. A differential scanning calorimeter with an enthalpy-step procedure using hermetically sealable pans to prevent vapor loss was used for measurements of specific heat capacity. Temperature calibration of the instrument for a previous study of aqueous sodium chloride was performed with indium, water, mercury, and adamantane. New calibration verification tests with indium and water showed deviations from the previous calibration no larger than the estimated temperature uncertainty of 0.08 K.

The enthalpy step technique involved an initial isotherm at 294 K, followed by an 8 K increase in temperature to an isotherm at 302 K. The area of the peak for the step multiplied by the calibrated cell constant is equal to the change in enthalpy,  $\Delta H$ . The change in enthalpy was divided by the temperature change and assigned as the heat capacity at the average temperature. Calibration of the cell constant for the above method was performed using sapphire (NIST SRM 720) and distilled, deionized water with electrical resistivity of approximately 18M $\Omega$ •cm.

### 2.2.2 Results

The measurement of the heat capacities for these solutions was cumbersome due to a reaction process inconsistently occurring within the solutions. The reaction process possibly could be release

of CO<sub>2</sub> for example. The solutions in their containers at ambient temperature showed a slight layer of foam on the surface. For different trials of each agent, different values of the heat capacity would be calculated, depending on whether the other reaction process did or did not occur. The enthalpy for the process would be added to the enthalpy from the temperature change making the heat capacity calculation invalid. For example, two trials of agent “B-1% solution” had  $c_{p,s}$  of 4.192 and 4.059 with uncertainties of 0.05. A third trial had a peak for the temperature change giving a heat capacity of 4.060. However, during the final isotherm at 302 K a second peak occurred from a chemical reaction process. This second peak area was added to the first with the invalid resulting heat capacity of 4.190. The above indicates the heat capacity value of 4.060 was correct. For all other trails, only one peak was seen so this reaction, when it occurred, proceeded during the temperature change. The magnitude of the enthalpy of the process appeared approximately identical for 1% concentrations of agents A and B and 3% concentrations of agent C but was larger for 3% concentrations of agent D. The above method was extended to include a temperature step from 302 K back to 294 K to check reversibility. The  $\Delta H$  for the step-up and step-down were always identical within experimental uncertainty indicating the reaction process was reversible. Experimental results showed the above process did not occur for the concentrated agent samples. Results of the measurements of the solutions are shown in Table 1.

**Table 1 Specific Heat of Fire Suppression Agents at Constant Pressure**

Sample	Temperature (K)	Specific Heat, $C_p$ (J/g K)	Uncertainty,d (J/g/K)
Tap Water	298.39	4.18	0.03
Agent A 1% solution	298.41	4.17	0.04
Agent B 1% solution	298.37	4.06	0.05
Agent C 3% solution	298.42	4.12	0.05
Agent D 3% solution	298.41	3.84	0.06
Agent A concentrate	298.55	2.95	0.04
Agent B concentrate	298.58	3.09	0.04
Agent C concentrate	298.56	3.64	0.05
Agent D concentrate	298.60	3.81	0.06

### 2.2.3 Conclusions

The measurements in Table 1 show the specific heat of all the agent solutions to be equal or less than the specific heat of plain water. Given that the specific heat of the concentrates, are significantly less than the specific heat of water, adding more concentrate would continue to reduce the heat absorbing capability of the solution. From this set of experiments it has been demonstrated that these agents do not increase water’s ability to absorb heat.

### 2.3 Fuel Cooling and Penetration

One of the advantages frequently cited for Class A agents is their ability to decrease the surface tension of water. Water has an inherently high surface tension. This characteristic causes water to bead and tend to roll off surfaces. It has been estimated that only 5 to 10 percent of the water applied during a fire attack contributes to the extinguishment [3]. The addition of a Class A concentrate

reduces the surface tension of the water and improves its ability to cover and penetrate surfaces.

The combination of improved penetration capability and foaming serves to increase the quantity of water retained on the surface of the fuel. This can potentially significantly increase the effectiveness of water during fire department mop-up operations. As part of this project, an experimental procedure was developed to evaluate the change in water penetration capability obtained through addition of Class A foam concentrates. Experiments were conducted to determine relative rates of penetration, rates of cooling, and areas of coverage.

An infrared imaging radiometer was used to examine penetration rate and measure surface temperatures. Thermal imaging radiometers produce photographs or other two dimensional records of the apparent temperature of surfaces. All objects radiate energy; the amount of energy radiated increases with increasing temperature. Objects at or near room temperature have spectral energy distributions that peak in the middle infrared region, near  $10\ \mu\text{m}$ . A sufficient amount of energy is radiated to allow detection at great distances by a sensitive instrument. The consistency of the relationship between object temperature and radiated energy allows a calibrated instrument to make highly accurate non-contact temperature measurements [4].

The earth's atmosphere absorbs radiated energy in the infrared except for two wavelength regions called atmospheric windows. Typically, it is water vapor in the atmosphere that absorbs the majority of the infrared energy over much of the spectral band. The atmospheric windows allow radiometric measurements with minimal losses. The  $8\text{-}14\ \mu\text{m}$  region is exceptionally free of absorption except with very high water content. The  $3\text{-}5\ \mu\text{m}$  region has relatively high transmission, but usually requires compensation when high accuracy measurements are to be made at path lengths greater than one meter. In addition, sun glint is a far more serious problem in the  $3\text{-}5\ \mu\text{m}$  waveband than in the  $8\text{-}14\ \mu\text{m}$  waveband. Modern thermal imaging radiometers are available with  $8\text{-}14\ \mu\text{m}$ ,  $3\text{-}5\ \mu\text{m}$ , or  $3\text{-}14\ \mu\text{m}$  spectral response. The system used in these experiments was of the third type [5].

The great advantage of thermal imaging radiometers is their ability to rapidly display changing conditions of a planar image. The device response time is on the order of nanoseconds while other typical non-contact thermometers require milliseconds to respond for a single point. A thermal imaging radiometer performs over 1 million measurements per second. With video recording and computer processing, tremendous amounts of thermal data can be archived, accessed, and analyzed. The major disadvantage of thermal imaging radiometers compared to other non-contact thermometers is their cost which is typically 20 to 30 times higher [6].

### **2.3.1 Experimental Procedure**

To evaluate the relative penetration capability, droplets of water and foam solution were simultaneously placed on the top side of a substrate. The response of the substrate was examined by viewing the bottom side with the infrared imaging radiometer. The thermal image obtained from the radiometer was recorded on videotape and analyzed using computer software. A diagram of the apparatus is shown in Figure 1.

After some trial and error, the optimum combination of droplet size, solution temperature, and substrate material was identified. Plain water and foam solution were placed on the substrate using

two hypodermic syringes each calibrated to deliver 100  $\mu\text{l}$ . This quantity of liquid was sufficient to provide a measurable response within the radiometer's field of view. To improve response and minimize the influence of extraneous variables, the water and foam solutions were chilled using an ice bath. The liquid temperature was typically 2  $^{\circ}\text{C}$  when placed on the room temperature (22  $^{\circ}\text{C}$ ) substrate.

A 0.2 m (7 in) square by 6.3 mm (1/4 in) thick hardboard was used as the test sample. Hardboard is one of several types of composition-boards, manufactured from wood elements ranging from veneers to fibers using one of several methods. The American Hardboard Association identifies hardboard as a board with a density of 480  $\text{kg}/\text{m}^3$  or greater. In the trade, however, a distinction is made between medium density fiberboard, often referred to as MDF, and higher-density fiberboard, called hardboard in the narrowest sense. The higher-density fiberboard typically has a density of 900  $\text{kg}/\text{m}^3$  or greater [7]. The hardboard used in these experiments had a density of approximately 960  $\text{kg}/\text{m}^3$ . In addition to providing consistent material properties, the relatively smooth surface of this material provided a good visual indicator of the impact of the surfactant.

The temperature span covered by the radiometer during a typical test was 2  $^{\circ}\text{C}$ . This span was increased to 5  $^{\circ}\text{C}$  for a few tests when the surface temperature dropped to within 0.2  $^{\circ}\text{C}$  of the original lower limit. The underside of the sample was painted with a flat black paint to minimize reflection, and control the emissivity at a value near 1. The temperature data was determined from the infrared images using software provided by the manufacturer of the radiometer. As recommended by the manufacturer, the system was operated at an emissivity setting of 1, and variations in emissivity were accounted for using the analysis software.

Prior to the start of each test, the temperature of the surface of the sample was recorded using a 0.25 mm (0.01 in) diameter Type K thermocouple embedded in the material surface. The liquid temperatures were determined using a glass bulb thermometer with 1  $^{\circ}\text{C}$  graduations. At application, the typical temperature difference between the liquid and the solid was approximately 20  $^{\circ}\text{C}$ .

### **2.3.2 Analysis**

A total of 17 tests were performed using four different Class A foam additives. The agents, identified as A, B, C, and D, were applied at their manufacturer's recommended concentrations. A 1% concentration was used for agents A and B while a 3% concentration was used for agents C and D. A test matrix indicating test number, foam concentrate used, and test duration is shown in Table 2.

**Table 2. Test Matrix**

Test Number	Agent	Duration of Test (min)	Initial Thermal Penetration Time (s)	
			Water	Agent
1	A	13	55	60
2	A	20	55	70
3	B	20	85	80
4	C	20	45	45
5	D	15	65	70
6	A	18	30	32
7	B	20	45	50
8	C	20	40	60
9	D	20	40	45
10	A	20	45	50
11	B	20	80	90
12	C	20	40	42
13	D	20	35	40
14	A	10	45	50
15	B	10	50	50
16	C	10	45	49
17	D	9	45	47

The rates at which the thermal effect of the agent solution and pure water penetrated the hardboard material were determined by measuring the time between placement of the liquids and appearance of initial cooling effect. Review of the infrared image videotapes indicates that the water and foam appear to penetrate hardboard at approximately the same rate. Typically, penetration rates were within 10 percent. The times for penetration of the water and agent are shown in Table 2. A significant portion of the variation in time is due to problems associated with simultaneously placing both drops on the hardboard. The average time required for initial penetration was about 50 s.

The relative rate at which each agent cooled the material was determined through analysis of the infrared images using the software provided by the radiometer manufacturer. The temperatures at points approximately in the center of the areas being impacted by the agent solution and the water were recorded as a function of time. To minimize the impact of emissivity, background temperature, and other variables, the temperature change was compared on a relative basis. Each data point was calculated by dividing the temperature change from ambient for the area cooled by the water into the temperature change for the area cooled by the agent. A value of 1 indicates the relative cooling rate was the same as water. Figures 2, 3, 4, and 5 present the results for Agents A, B, C, and D, respectively.

With the exception of Agent A, most of the data appears reasonably consistent between replicate tests. After about 3 minutes, the agent cooling rate begins to exceed that of the water. Over the course of a test utilizing a surfactant, the average cooling rate is about 1.5 times that of the water. The 3 minute delay would suggest that the primary reason for the improved cooling is the larger area covered by the agent solution. When placed on the hardboard material, all of the agent solutions

would immediately spread across the surface. This is a direct result of the surfactant contained in the Class A foam additives. The water would remain as a single droplet on the surface. Typically, a significant quantity of water would remain beaded on the surface at the conclusion of a 20 minute test. In most cases, the agent solution would have disappeared from the surface as a result of absorption and evaporation.

The final piece of information obtained from the infrared data was relative area thermally effected by the agent solution versus the water. The ratio of agent on the bottom surface to that of water is summarized for the four agents in Table 3.

**Table 3. Relative Area of Coverage**

<b>Agent</b>	<b>Test Number</b>	<b>Relative Area of Thermal Impact</b>
A	1	3
	2	4
	6	3
	10	5
	14	3
	Average	3.6
B	3	6
	7	4
	11	4
	15	4
	Average	4.5
C	4	3
	8	5
	12	4
	16	4
	Average	4
D	5	4
	9	4
	13	2
	17	5
	Average	3.7

One of the features of the infrared analysis software is the ability to apply a direct measure scale to the area being viewed. The software uses the configuration of the experiment together with certain optical properties of the radiometer to determine appropriate length measurements. Using this feature and some of the other measurement tools, the ratio of area cooled by the agent solution to that cooled by the water was determined for each test. A higher number indicates that the agent solution had a greater area of impact. In all cases, the foam had an apparent area of impact at least twice that of the water with 4 times being typical.

### **2.3.3 Conclusions and Recommendations**

Using infrared thermography techniques, it was possible to examine several of the properties potentially important in evaluating the fire fighting effectiveness of Class A foam additives. These properties dealt primarily with the surfactant contained in the agents and its impact on the surface tension of the water. The initial penetration time was the same for both the plain water and the water - Class A agent solution. The agents were shown to have measurably increased relative rates of cooling and areas of impact compared to water. The four agents investigated appear to have about the same impact on the wetting properties of water as determined through the infrared data.

A number of issues need further investigation and resolution before infrared thermography can be recommended as part of a standardized test for Class A agents. Changes in the measurements over the small temperature range, about 2 °C, can produce significant variations in the results. Methods need to be investigated to increase the temperature ranges without introducing additional variables such as cracking of the material surface and smoldering. Simultaneous placement of droplets on the surface is critical to conducting directly comparative measurements. An apparatus appropriate for this task must be developed. In addition, implications of and methods for placing multiple drops on surfaces must be examined.

## **2.4 Fuel Surface Contact**

When an agent is in contact with the surface of a hot fuel, it is transferring heat by conduction. Heat transfer is only occurring at the interface of the fuel and the agent. If the agent has a high surface tension like water, 75 dynes/cm [8], most of the agent will be beaded up, limiting the surface area of contact. If the agent has a lower surface tension, the agent will spread on the fuel surface, increasing the contact area and the heat transfer (Figure 6).

Measuring the contact angle of a drop of liquid on a fuel surface can be used to quantify wettability and surface contact. The contact angle is the angle between the surface and the tangent line at the point of contact. If complete wetting occurs, i.e. maximum surface contact is approached, then the contact angle will approach 0°.

### **2.4.1 Experimental Procedure**

A contact angle meter with a range from 10° to 120° was used for these experiments. Substrate materials included glass, stainless steel, material from the sidewall of an automobile tire, unstained T1-11 plywood siding, stained T1-11 plywood siding and a high density hardboard. Similar volume droplets were placed on the substrate with a micro dispenser with 5 ml pipette tubes. Separate pipette tubes were used with each agent to avoid cross contamination. A contact angle reading was made within a few seconds of the droplet being placed on the surface.

The substrates were carefully handled and prepared to avoid fingerprints or other contaminants from contacting the surfaces. The glass microscope slide covers were taken from sealed packages and used without further cleaning. The stainless steel was polished with very fine crocus cloth, washed off with tap water and dried with a paper towel. Then the test surface was washed with acetone and blown dry with “dry” compressed air. The tire sidewall was washed off with water to remove grit and residue from cutting the sample from the tire. The unstained plywood siding was cut from a

sheet of plywood as delivered from a lumber yard; the moisture content was less than 10%. The stained plywood sample had one coat of waterproofing stain applied with a roller. The amount of stain applied averaged 265 g/m<sup>2</sup> over the 1.22 m x 2.44 m panel from which the sample was cut. The sample cured for approximately 6 months. The stain meets federal specification TT-W-572B for water repellency on wood. The hardboard sample is medium density hardboard with a density of 960 kg/m<sup>2</sup>. The hardboard was wiped with a clean, dry cloth prior to testing to remove any sawdust.

In addition to the tap water and agent samples, distilled and deionized water was also used for the contact angle experiments. All of the solutions were made from tap water. The agent solutions were mixed within 24 hours of use in the experiments.

#### 2.4.2 Results and Discussion

Each combination of agent and substrate had a least three replicate experiments performed. The results shown in Table 4 are the averages of the replicate experiments. The uncertainty of the contact angle measurement device is  $\pm 0.5^\circ$ .

**Table 4 Contact Angle Measurements**

Agent	Substrate					
	Glass	Stainless Steel	Tire	Unstained Plywood	Stained Plywood	Hardboard
D/D Water	42.4	88.0	80.0	~	98.7	100.4
Tap Water	50.4	86.8	81.6	~	106.7	99.6
Agent A 1%	25.3	14.0	18.8	~	◆	X
Agent B 1%	37.3	11.3	16.0	~	◆	X
Agent C 1%	29.0	<10	16.4	~	◆	X
Agent D 1%	27.8	<10	31.6	~	◆	X
Agent C 3%	32.2	<10	19.2	~	◆	X
Agent D 3%	30.2	<10	25.6	~	◆	X
Agent C 6%	31.1	10.7	22.8	~	◆	X
Agent D 6%	31.8	<10	19.6	~	◆	X

~ Completely absorbed into unstained plywood within 5 seconds after application.

◆ Completely absorbed into stained plywood within 30 seconds after application.

X Completely absorbed into hardboard within 15 seconds after application.

With the exception of the unstained plywood, water in both distilled and tap form, beaded up on top

of the substrate. In the case of the unstained plywood, the water and the agent solutions were absorbed or penetrated into the wood within seconds of application. All of the agents demonstrated significantly lower contact angles relative to water on the impenetrable surfaces and penetrated surfaces, stained plywood and hardboard, which water could not.

Stainless steel was used as benchmark to compare with a study on droplet evaporation by Qiao et. al.[9,10]. This study examined the effect of evaporation of drops placed on a hot stainless steel plate. Contact angles were used to characterize the droplets. The contact angles were varied by adding a surfactant, sodium dodecyl sulfate, to the water. The results state, "As the liquid layer becomes thinner, heat transfer from the solid to the liquid-vapor interface is enhanced. Spreading of the droplet also increases the heat transfer area. Both of these effects contribute to a faster evaporation rate: decreasing the contact angle from 90° to 20° reduced the droplet evaporation time by approximately 50%"[10]. In other words, the water/surfactant solution provided twice the cooling as plain water. Table 4 shows the baseline water contact angles to be approximately 90° and the agents all have contact angles less than 20°. Therefore, based on these contact angle tests and Qiao's results, an increased cooling capability of a factor or two would be expected from these agents.

### **2.4.3 Conclusions**

The surfactants in Agents A,B,C and D significantly reduce the contact angle of their solutions relative to plain water. This increases the surface area covered by a single droplet and based on previous studies should increase the rate of cooling.

## **2.5 Droplet Size**

Heat transfer is very important in suppressing fires. Heat transfer is dependent on many mechanisms, such as: the ability of materials to absorb heat, the difference in temperature and the surface area. An example of a ventilation limited room fire is a sofa burning and flames starting to come out of the window. In this case, the agent's capability, based on specific heat, to absorb heat is similar to water and the temperature differences would be the same with an agent or water. The heat transfer will vary as a function of surface area. When a fire suppression agent is discharged into the room it can transfer heat from the hot gases or flames, the surfaces in the room, and the burning sofa.

When the agent is delivered as a straight steam, its surface area is small when it passes through the flames. Therefore almost all of the agent will hit a surface, break up and splash. If the surface is hot, the agent will start absorbing the heat. So the heat transfer is limited by the area of the hot surfaces in the room. If the water hits the burning item or the ceiling, steam will be generated to displace oxygen in the room and help knock down the fire.

If the agent is delivered as a spray, the surface area of the agent will increase dramatically. If the drops are small enough, significant amounts of heat can be transferred while the agent is passing through the flames and hot gas. This scenario can provide faster steam conversion and a very rapid fire knockdown compared to straight stream application.

Discharging agent into a room, in the form of a 51 mm (2.5 in) stream provides a surface area of 0.24m<sup>2</sup> (370 in<sup>2</sup>) per gallon prior to the stream impacting on a surface. If the agent is discharged as

a stream of large drops, 2 mm (0.078 in) in diameter, then surface area of the water per gallon increases almost 50 times to 11.4 m<sup>2</sup> (17,700 in<sup>2</sup>). If the diameter of the drops were reduced to 1 mm, the surface area of the agent available for heat transfer would double over that for 2 mm drops. This illustrates the relationship between surface area available for heat transfer and droplet size.

Water has a relatively high surface tension of 75 dynes/cm [8]. A high surface tension means that water is cohesive, it likes to stick to itself. This high surface tension causes water to bead up into large drops.

One of the properties of water which the agents affect is surface tension. This means the agents are surface active agents or surfactants. The addition of a surfactant reduces the surface tension of water. This will potentially allow the solution, when sprayed through a fire fighting fog nozzle, to break into smaller droplets resulting in more surface area of the solution being exposed to the fire.

The increased surface area provides greater heat transfer and heat loss from the fire. The greater the heat transfer/heat loss rate, the faster the fire will be extinguished. Due to their lower surface tension, droplets surviving beyond the flames, onto the fuel source, will be able to penetrate the fuel easier, extinguishing the fire more rapidly.

To investigate the impact of the agents on droplet size, droplet differences between water and water plus one of four surfactant agents (identified as agents A, B, C, and D) discharged from a hose were measured using a droplet analyzer. Droplet measurements were recorded at four different locations within a circular spray pattern. Droplet sizes, distribution and velocity were determined, averaged and compared. Finally, the percent differences were calculated.

### **2.5.1 Experimental Procedure**

An optical array laser probe was used to record the droplet measurements. This laser probe uses a process called the shadowing principle to obtain droplet measurements. The beam of the probe laser is reflected between the area of the two appendages of the probe (known as the measurement volume) through which the droplets pass, Figures 7 and 8. As the beam passes through this volume, it is reflected onto a diode array. Droplets passing through the laser create a shadow on the diode array. The width and scan times are recorded to form the dimensions of the droplet. Data obtained from the probe was recorded on a personal computer using the image analysis software provided with the probe.

The probe's software and hardware contain functions for error correction and droplet verification. Images of multiple droplets and droplets that do not fall completely in the measuring area are rejected. Droplets sizes from 30 μm to 1860 μm in diameter can be measured and recorded by the probe. Droplet measurements are put into class groups of 30 μm.

A typical fire fighting fog nozzle, capable of flowing between 0.6 l/s (10 gpm) and 1.9 l/s (30 gpm), was used to produce the droplets. The nozzle was capable of being adjusted from a straight stream to a full fog pattern of approximately 90°. Foam solutions were either batch mixed and delivered through a portable centrifugal pump or proportioned using a bladder tank and the building standpipe system. Solutions were delivered to the nozzle through 30.5 m (100 ft) of 38 mm (1.5 in) diameter lined fire hose at a nozzle pressure of 690 kPa (100 psi).

The fog nozzle was secured above the ground at a height of 3 m (9.8 ft). It was oriented at a 90° angle to the floor, spraying downward. This produced a circular spray pattern parallel to the floor, Figure 7. The exact center of the spray pattern was located and marked on the floor. The spray pattern was adjusted to an approximate 15° degree angle with a radius of 0.3 m (1 ft) at a distance of 2.5 m (8 ft) from the nozzle. Throughout the remainder of the test series, the nozzle was not adjusted or moved in order to ensure identical results. However, a final test was conducted with the nozzle set to provide a full fog pattern.

The probe was mounted onto a movable platform with the laser sampling area 0.5 m (1.6 ft) above the floor and 2.5 m (8 ft) below the nozzle. The platform was positioned with the probe in the desired test location and measurements were recorded at positions 0 m, 0.1 m, 0.2 m, and 0.3 m radially from the centerline. Selected measurements were taken to ensure that a symmetrical pattern was obtained from the nozzle.

Tests were conducted using water and each of the four solutions for a minimum of 1200 seconds at each location within the spray pattern. Since the water was obtained directly from the building standpipe, the tests using plain water were completed in single, continuous 1200-second runs at each location. Agents A and B, mixed at 1%, were proportioned using the bladder tank. Because of the size of the bladder tank, the tests could only be run for a maximum of 600 seconds. Three 600-second tests were conducted for each location. Agents C and D, mixed at 3%, were batch-mixed in a tank and than pumped to the nozzle using a portable fire pump. The size of the tank allowed for tests that could run for a total of 1200 seconds. One 1200-second test was conducted at each location. One test using water with the nozzle set to the full fog pattern was conducted to examine the impact of the nozzle alone on droplet size. A flow rate of approximately 0.6 l/s (10 gpm) was used in all of the tests.

### 2.5.2 Analysis

Analysis of the data obtained from this test series was conducted using ASTM E 799-92, Standard Practice for Determining Data Criteria and Processing for Liquid Drop Size Analysis [11] as a guide.

There are several values of interest in characterizing liquid drop size distributions. The volume median diameter or average droplet size is defined as the drop diameter such that 50% of the total liquid volume is in drops of smaller diameter,  $D_{v0.5}$ . The drop diameter such that 90% of the total liquid volume is in drops of smaller diameter is identified as the  $D_{v0.9}$ . The drop diameter such that 99% of the total liquid volume is in drops of smaller diameter is the  $D_{v0.99}$ . In addition, the average length/width ratios and velocities were calculated. For the final analysis, all values from the multiple tests were averaged. The  $D_{v0.5}$ ,  $D_{v0.9}$ , and  $D_{v0.99}$  for each solution at each location are shown in Tables 5, 6, and 7, respectively.

**Table 5.  $D_{v50}$  ( $\mu\text{m}$ ) Data for Water and Four Agents at Four Measurement Positions**

Position	Water	Agent A	Agent B	Agent C	Agent D
Centerline	309	297	325	287	252
0.1 m	300	266	291	275	277
0.2 m	260	296	300	278	278
0.3 m	289	299	354	253	266

**Table 6.  $D_{v90}$  ( $\mu\text{m}$ ) Data for Water and Four Agents at Four Measurement Positions**

Position	Water	Agent A	Agent B	Agent C	Agent D
Centerline	573	626	663	516	464
0.1 m	523	484	509	426	439
0.2 m	421	517	453	464	445
0.3 m	485	501	538	448	441

**Table 7.  $D_{v99}$  ( $\mu\text{m}$ ) Data for Water and Four Agents at Four Measurement Positions**

Position	Water	Agent A	Agent B	Agent C	Agent D
Centerline	906	805	1276	877	735
0.1 m	824	806	864	575	602
0.2 m	656	813	590	597	622
0.3 m	638	683	802	639	639

In order to normalize the data for comparison with water, the  $D_v$  values of water were divided into all the values. This gave water a value of one at every location. Agents that have a  $D_v$  value larger than water are greater than one, agents with  $D_v$  values less than water have are less than one. The normalized results are presented in Tables 8, 9, and 10. The average percent difference between water and each agent was calculated and shown in the last row in each Table. The estimated error was one size class of 30  $\mu\text{m}$ . The error used for calculating percentage error was  $\pm 15 \mu\text{m}$ . The droplet size tests conducted on water gave a  $D_{v0.99}$  value of 756  $\mu\text{m}$ . The  $D_{v0.99}$  values of agent A and B were both larger than water while the  $D_{v0.99}$  values of agent C and D were smaller.

**Table 8. Normalized  $D_{v50}$  ( $\mu\text{m}$ ) Data for the Four Agents at Four Measurement Positions**

Position	Agent A	Agent B	Agent C	Agent D
Centerline	0.96	1.05	0.93	0.82
0.1 m	0.89	0.97	0.92	0.92
0.2 m	1.14	1.15	1.07	1.07
0.3 m	1.03	1.22	0.88	0.92
Percent Diff.	0.52	10.01	-5.25	-6.79

**Table 9. Normalized  $D_{v90}$  ( $\mu\text{m}$ ) Data for the Four Agents at Four Measurement Positions**

Position	Agent A	Agent B	Agent C	Agent D
Centerline	1.09	1.16	0.90	0.81
0.1 m	0.93	0.97	0.81	0.84
0.2 m	1.23	1.08	1.10	1.06
0.3 m	1.03	1.11	0.92	0.91
Percent Diff.	6.97	7.89	-6.48	-9.61

**Table 10. Normalized  $D_{v,99}$  ( $\mu\text{m}$ ) Data for the Four Agents at Four Measurement Positions**

Position	Agent A	Agent B	Agent C	Agent D
Centerline	0.89	1.41	0.97	0.81
0.1 m	0.98	1.05	0.70	0.73
0.2 m	1.24	0.90	0.91	0.95
0.3 m	1.07	1.26	1.00	1.00
Percent Diff.	4.41	15.33	-10.56	-12.71

Agent A created significant amounts of foam and appeared to be a foaming agent. The turbulence created as the solution passed through the fog nozzle appeared to induce a foaming action. The foams were thick and lasted for several hours before breaking down. The spray pattern was not altered by the solution and it flowed at a rate comparable to water. Agent B also created large amounts of foam similar to agent A. Agent C created very little foam when tested. It did not alter the spray pattern and flowed at a rate comparable to agents A and B. Agent D also did not foam and was unique in that it flowed at a much higher rate than the other three agents under identical conditions. It is possible that agent D lowered the viscosity, which decreased friction loss in the hose, but this can not be verified without additional testing. Agent D appeared to foam less than the other agents during these experiments.

Agent A had a  $D_{v,99}$  of 776  $\mu\text{m}$ . This size difference of 20  $\mu\text{m}$  turned out to be less than one class size (30  $\mu\text{m}$ ) larger than water. With a size difference so small, it would seem that the solution characteristics would be similar to water. However, Agent A had a velocity 1.17 m/s slower. The velocity data obtained for water and the four agents is summarized in Table 11. A comparison of Agent A to water indicates that Agent A produces larger, lighter, and slower moving droplets.

**Table 11. Velocity in m/s for Water and the Four Agents at Four Measurement Positions**

Position	Water	Agent A	Agent B	Agent C	Agent D
Centerline	5.00	5.90	5.80	4.50	3.60
0.1 m	3.50	3.20	3.60	3.30	3.00
0.2 m	3.20	0.97	1.70	2.60	3.60
0.3 m	3.40	0.35	0.18	2.30	5.00
Average	3.78	2.61	2.82	3.18	3.80

Agent B had a  $D_{v,99}$  value of 883  $\mu\text{m}$ . This represents a difference of 127  $\mu\text{m}$  or over 4 size classes larger. It is the greatest difference of any of the agents tested. Agent B also changed the spray pattern into a much smaller angle and produced foam with a velocity approximately 1 m/s slower. When compared against water, agents A and B both performed about the same. Agent B produced droplets much larger than water with a low velocity.

The testing of Agent C resulted in a  $D_{v,99}$  of 672  $\mu\text{m}$  with droplets 84  $\mu\text{m}$  smaller and velocities 0.6 m/s slower than water. The loss in speed could be a result of energy loss from the forming of the smaller droplets. Additionally, the smaller droplets would have less mass and momentum and could be slowed more by the air. The smaller droplets of Agent C are unlike the droplets of agents A and B in that Agent C did not create foam or foam droplets. This translates into smaller water-like

droplets. This decrease in droplet size can increase the surface area of solution exposed for heat transfer. The smaller droplets coupled with the slower speed may result in more steam and less penetration.

Agent D produced the smallest of all the droplets with a  $D_{v0.99}$  of 649  $\mu\text{m}$ . This represents a difference of 106  $\mu\text{m}$ , which is more than 3 size classes. Agent D was unique in that it increased droplet velocity. Agent D flowed at a higher rate than the other surfactants, and produced a droplet velocity 0.02 m/s faster than water. Although the difference is small compared to water, it is an average of 1 m/s faster than the other three surfactants. The result is a smaller droplet at approximately the same velocity as water.

The comparison of the water at a 15° angle to a full fog pattern showed that solely using the nozzle, with no additive, the water droplet size could be decreased from a  $D_{v0.99}$  of 756  $\mu\text{m}$  to a  $D_{v0.99}$  of 600  $\mu\text{m}$ . The velocity of the smaller drops was lowered to 2 m/s; this is 1.78 m/s slower. In the comparison with water plus agents to water alone, droplet size was smallest when water alone was sprayed through the nozzle at a full fog pattern. The fog nozzle data is shown in Table 12.

**Table 12. Summary of Data for a Typical Fog Nozzle**

Cone Angle	$D_{v50}$	$D_{v90}$	$D_{v99}$	Velocity (m/s)
15	289	501	756	3.78
90	353	479	600	2.00
Percent Difference	21.97	-4.40	-20.6	—

**2.5.3 Conclusion**

From the perspective of this experiment, which was to demonstrate the effect of surfactant agents on water, Agent D produced the smallest droplets. Its smaller droplets, with no loss in velocity, would theoretically prove more efficient in transferring heat in the hot gas layer. However, the effectiveness of these agents on different types of fires can only be determined through additional testing on actual fires.

Further research should be conducted with single droplet generators to eliminate the variability of the nozzle. An additional project should be conducted to examine the effect of surfactant agents on drop size, pattern, and throw when applied through adjustable fog nozzles at higher fire fighting flow rates 6 to 16 l/s (100 to 250 gpm).

**2.6 References**

1. Friedman, Raymond, Theory of Fire Extinguishment, National Fire Protection Handbook 17th ed., Section 1/Chapter 6, Art Cote Ed., National Fire Protection Association, Quincy, MA. 1991.
2. Wahl, Andrew M., Water and Water Additives for Fire Fighting, National Fire Protection

- Handbook 17th ed., Section 1/Chapter 6, Art Cote Ed., National Fire Protection Association, Quincy, MA. 1991.
3. Principles of Foam Fire Fighting, Michael Wieder, Carol M. Smith, and Cynthia Brakhage, ed., Fire Protection Publications, Oklahoma State University, Stillwater, Oklahoma, 1996.
  4. Thermal Radiation Heat Transfer, Siegel, Robert and Howell, John R., McGraw-Hill Book Company, New York, New York, 1981.
  5. Model 760 IR Imaging Radiometer - Operators Manual, Inframetrics, Inc., North Billerica, Massachusetts, 1991.
  6. Measurement Systems - Application and Design, Doebelin, Ernest O., McGraw-Hill Book Company, New York, New York, 1983.
  7. Concise Encyclopedia of Wood and Wood-Based Materials, Schniewind, Arno P., ed., Pergamon Press, Oxford, England, 1989.
  8. Vargaftik, N.B., et.al., International tables of the surface tension of water, J. Phys. Chem. Ref. Data, 12, 817, 1983.
  9. Qiao, Y.M. and Chandra, S., A Evaporative Cooling Enhancement by Addition of Surfactant to Water Drops on a Hot Surface, ASME HTD Vol. 304-2, pp. 63-71, (1995).
  10. Chandra, S., di Marzo, M., Qiao, Y.M., Tartarini, P., AEffect of Liquid-Solid Contact Angle on Droplet Evaporation@, Sparse Water Sprays in Fire Protection, di Marzo, M.,ed., NIST-GCR-96-687. Nat. Inst. Of Stds & Tech., Gaithersburg, MD, June 1996.
  11. ASTM E 799-92, Standard Practice for Determining Data Criteria and Processing for Liquid Drop Size Analysis, American Society for Testing and Materials, Philadelphia, PA, 1992.

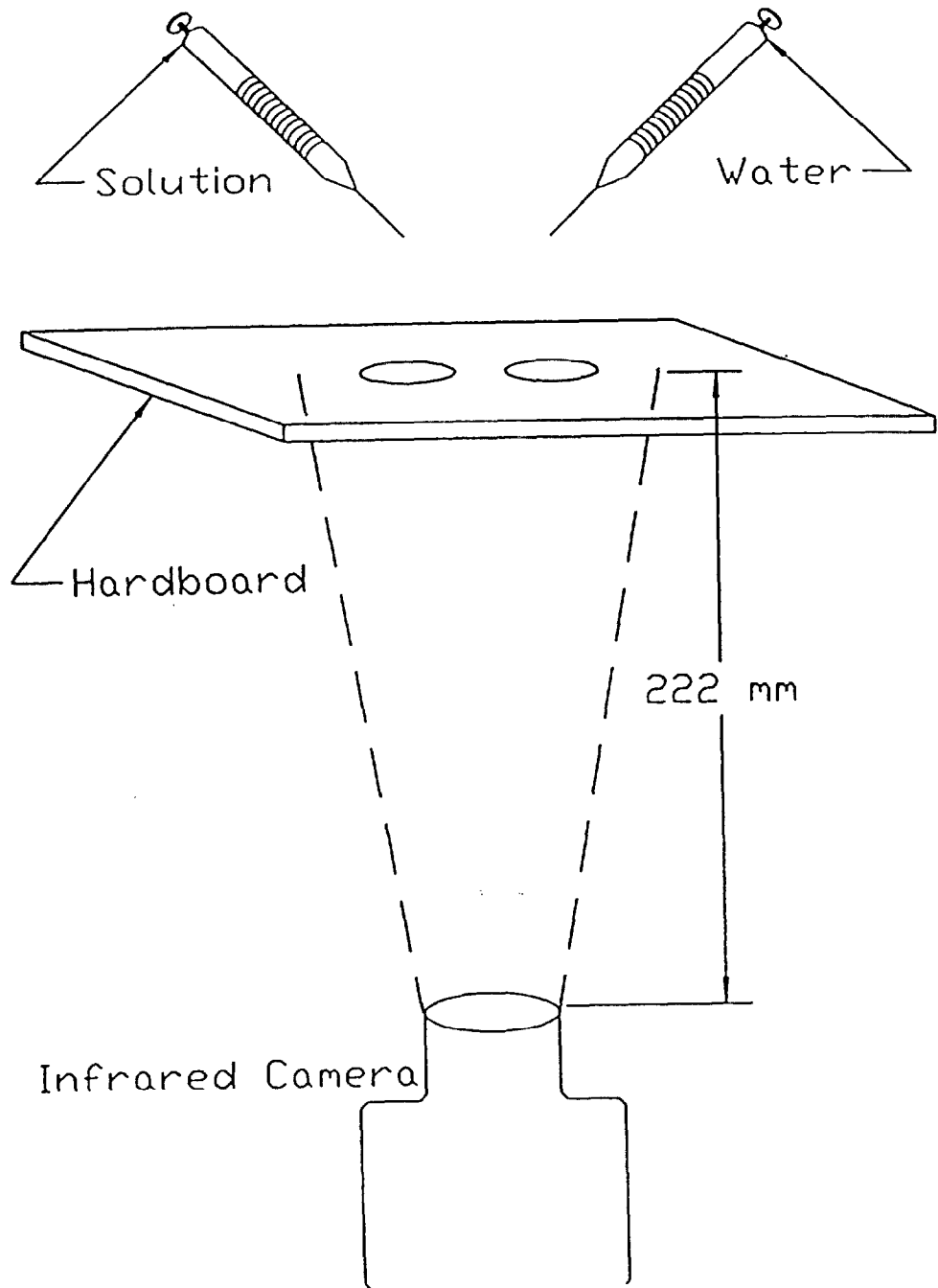


Figure 1. Diagram of Experimental Arrangement

# Agent A

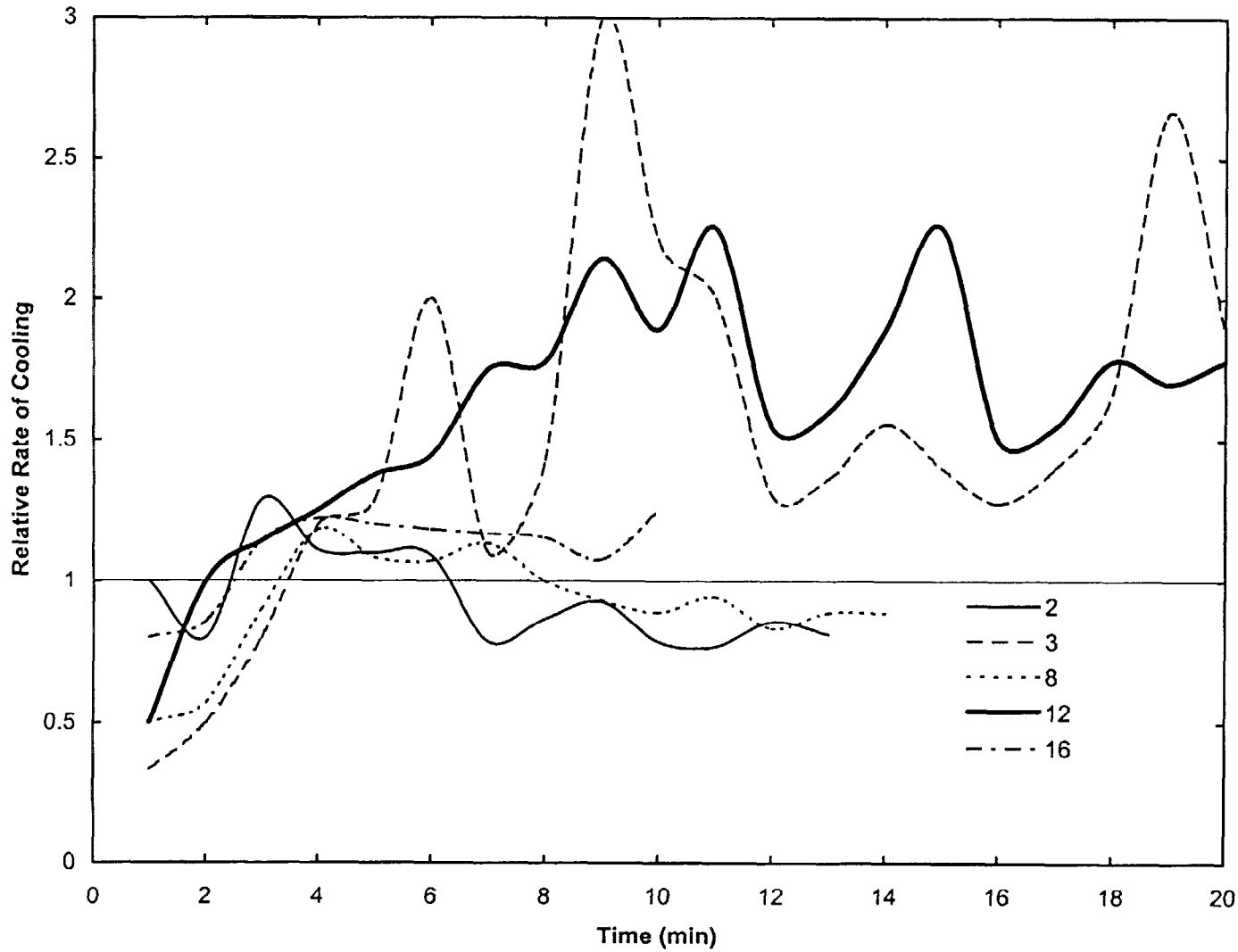


Figure 2. Rate of cooling relative to water, Agent A.

Agent B

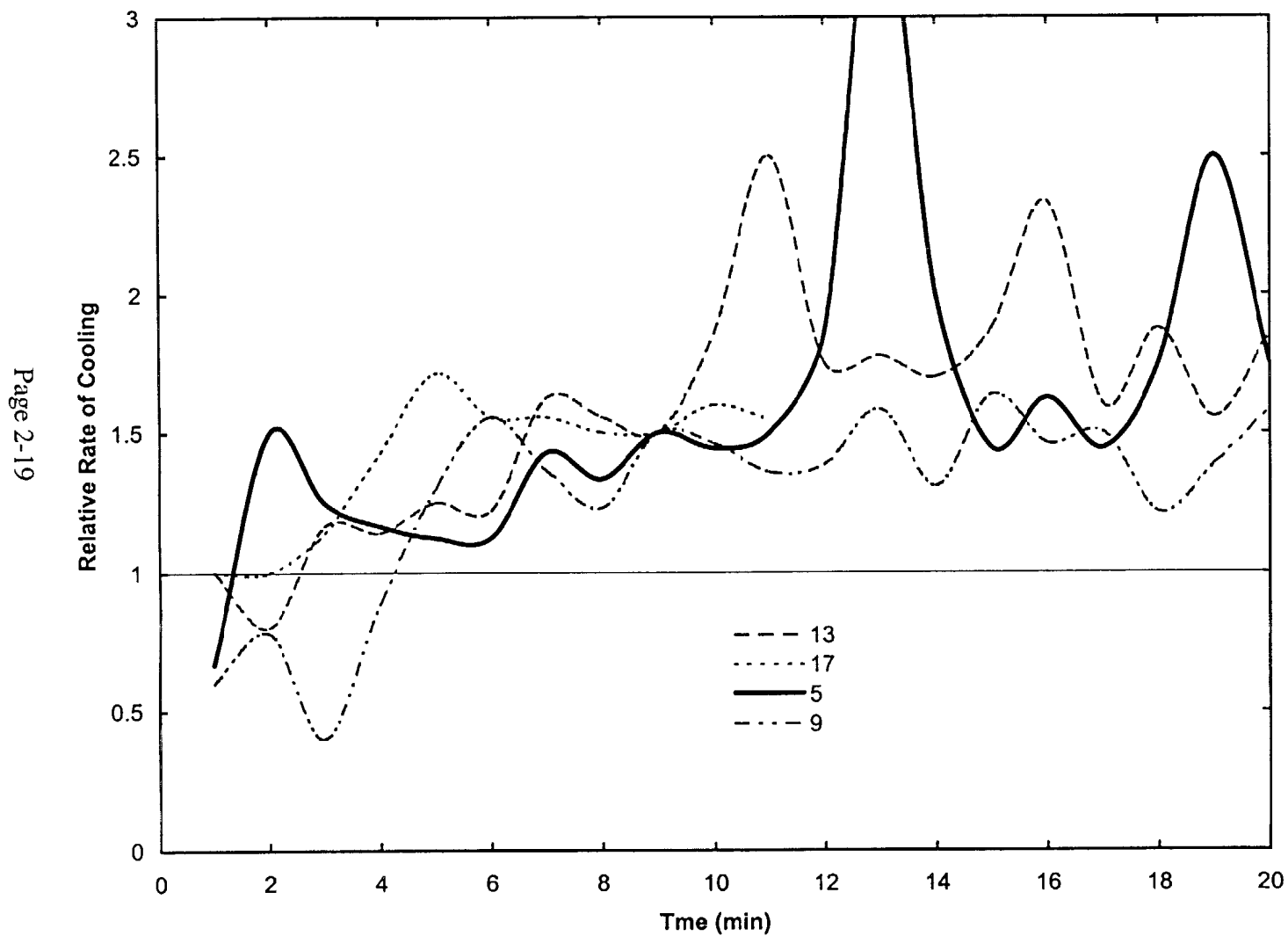


Figure 3. Rate of cooling relative to water, Agent B.

Agent C

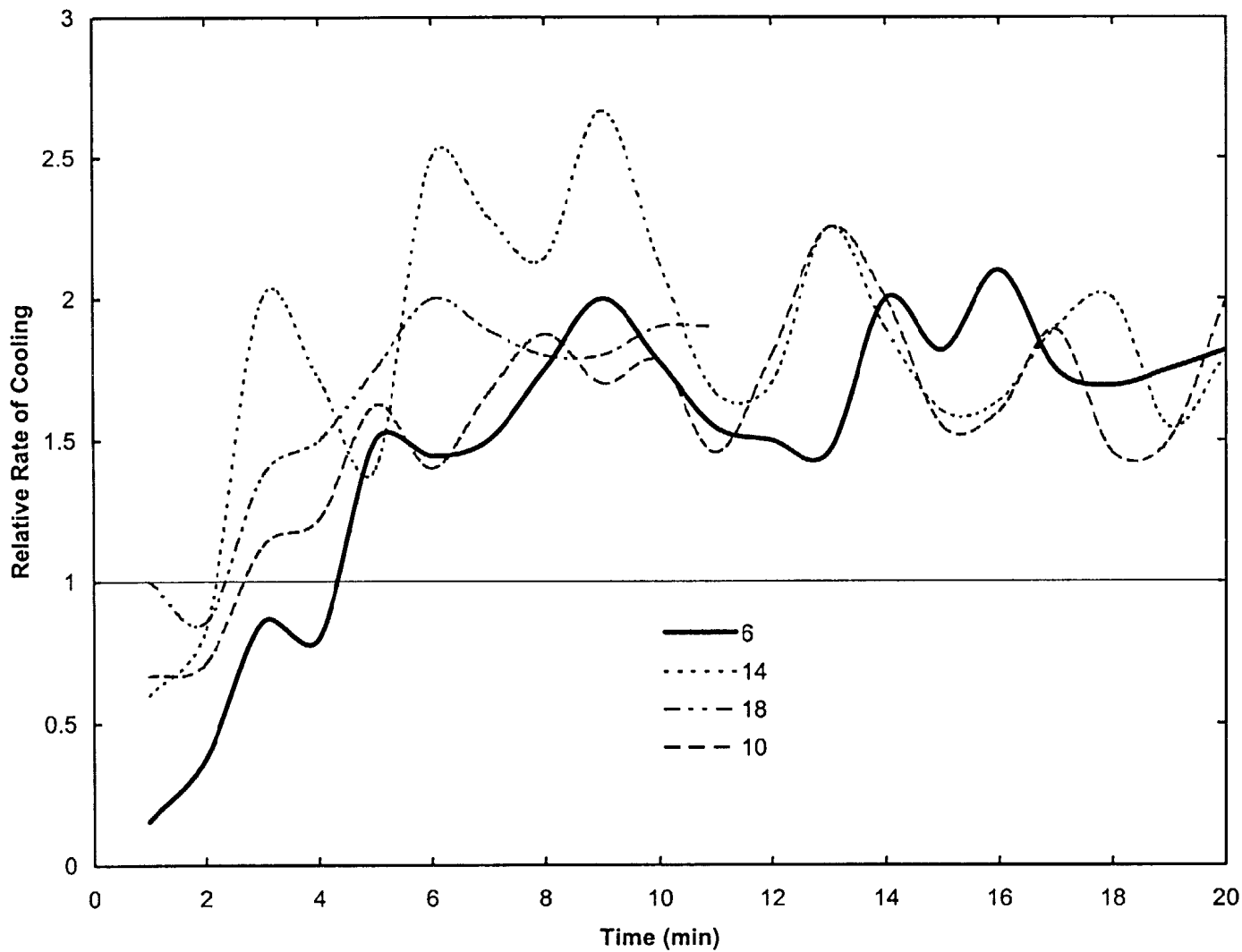


Figure 4. Rate of cooling relative to water, Agent C.

### Agent D

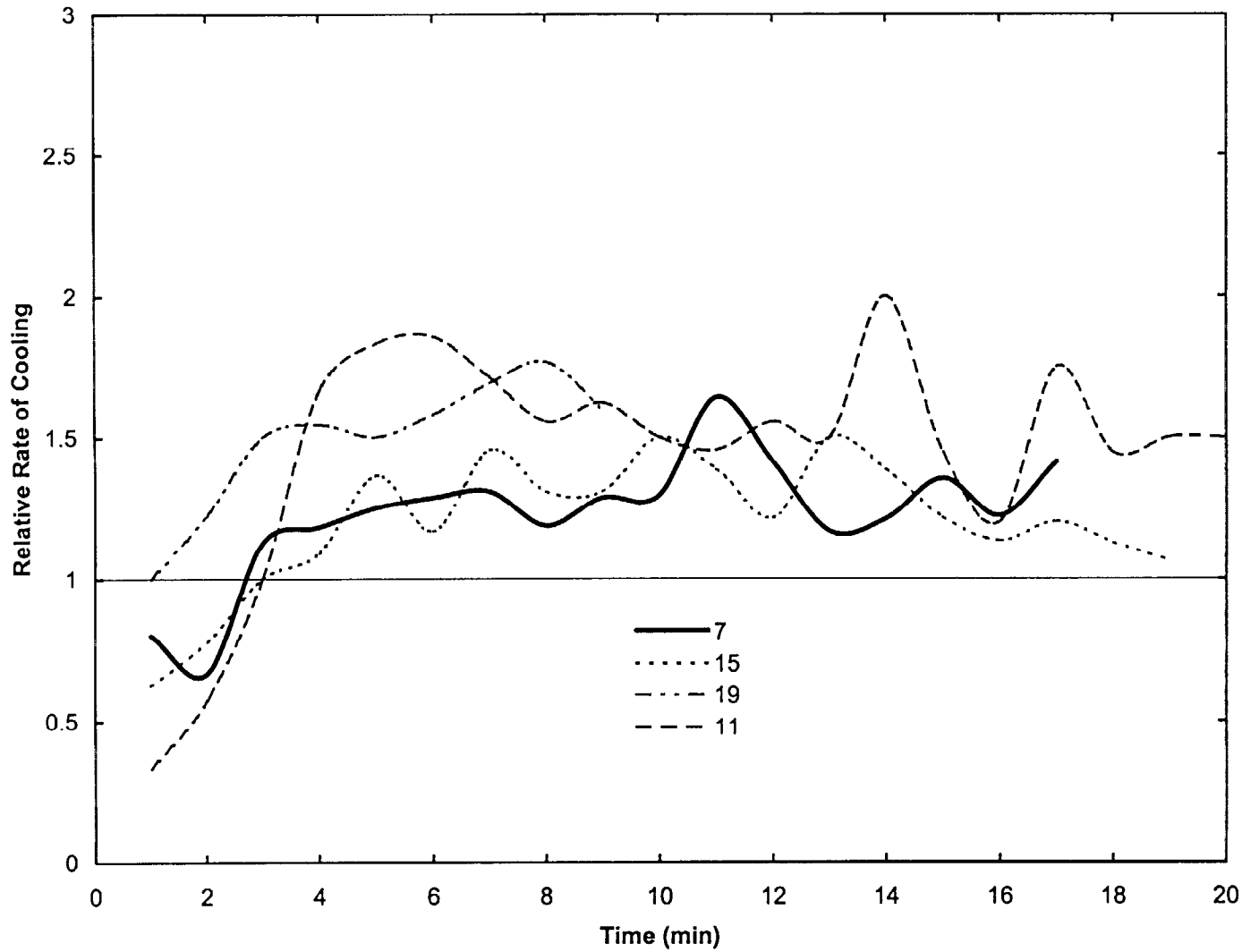


Figure 5. Rate of cooling relative to water, Agent D.

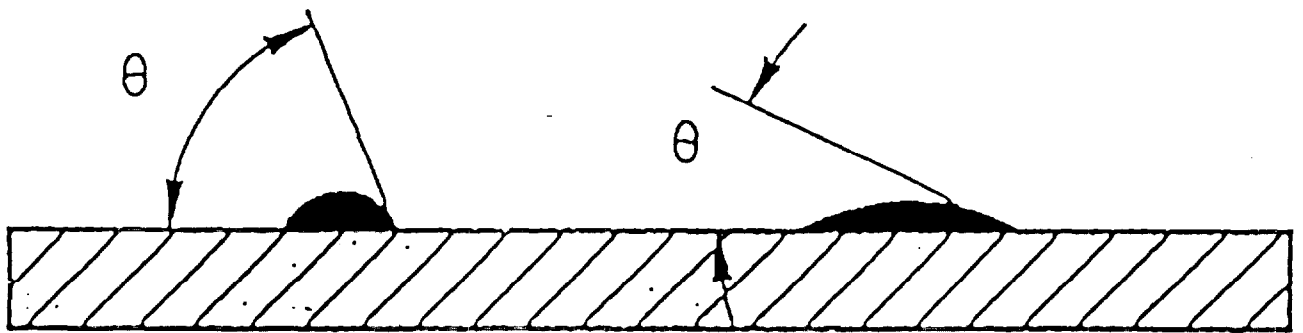
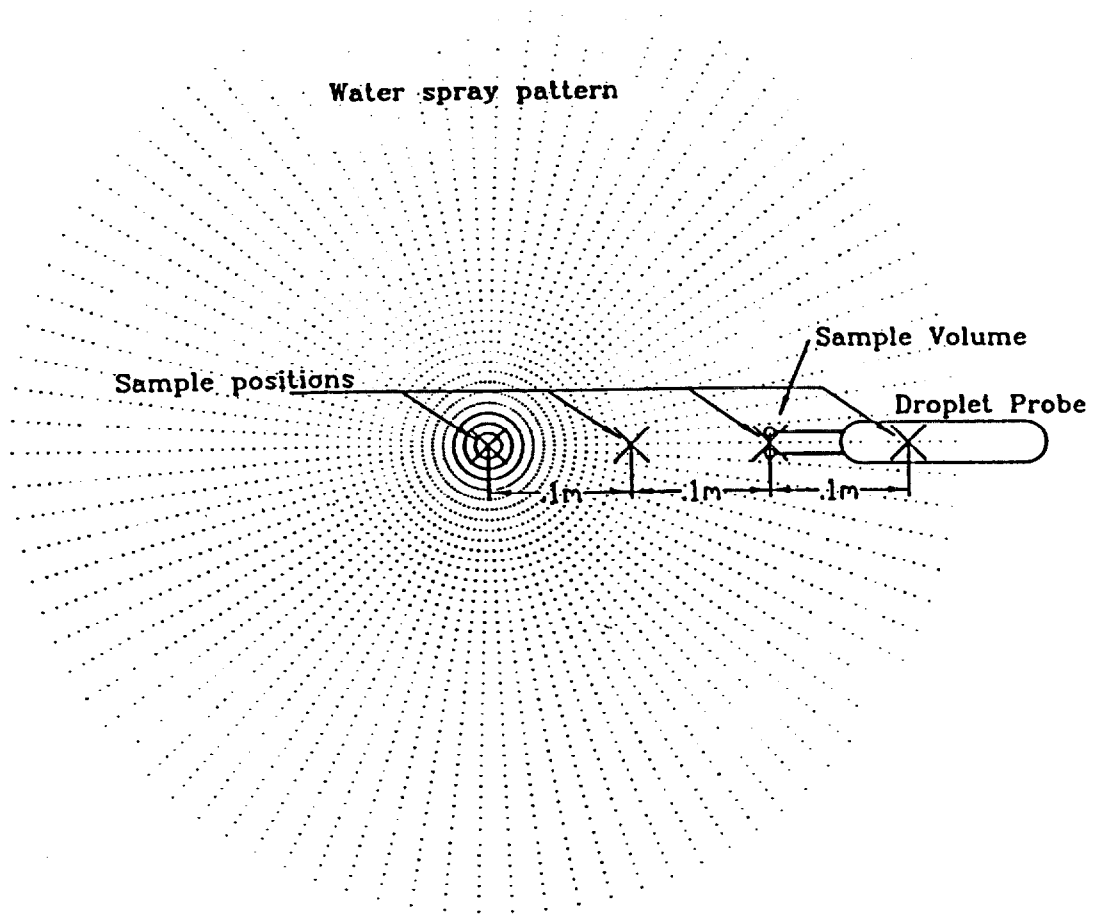


Figure 6. Diagrams of contact angle,  $\theta$

Plan View Above Nozzle



Measurements were taken at the center, .1m, .2m, and .3m as shown.

Figure 7. Plan view of droplet measurement arrangement.

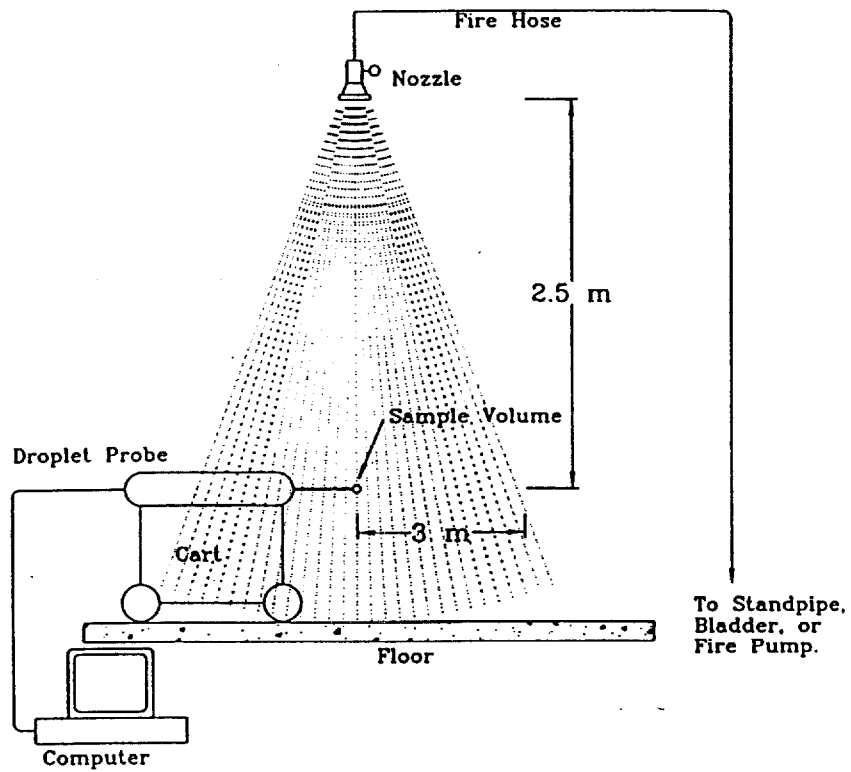


Figure 8. Elevation of droplet measurement arrangement.